PHYSICAL REVIEW D **92,** 094025 (2015)

Top quark chromoelectric and chromomagnetic dipole moments in a two Higgs doublet model with *CP* violation

R. Gaitán[*]
Departamento de Física, FES-Cuautitlán, UNAM, C.P. 54770, Estado de México, México

E. A. Garcés[†]
Departamento de Física, FES-Cuautitlán, UNAM, C.P. 54770, Estado de México, México and Instituto de Física, Universidad Nacional Autónoma de México, Apartado Postal 20-364, 01000 México DF, México

J. H. Montes de Oca[‡]
Departamento de Física, FES-Cuautitlán, UNAM, C.P. 54770, Estado de México, México

R. Martinez[§]
Departamento de Física, Universidad Nacional de Colombia, Bogotá Distrito Capital, Colombia
(Received 29 May 2015; published 25 November 2015)

In this work we study the anomalous top quark-gluon couplings chromoelectric dipole moment and chromomagnetic dipole moment in a general two Higgs doublet model with *CP* violation. We find that this model provides an important contribution from the Y_{tt} Yukawa coupling that needs to be taken into account. The predictions for the chromomagnetic dipole moment and chromoelectric dipole moment obtained are $-0.03 < \Delta\tilde{k}_t < -0.005$ and $|\Delta\tilde{d}_t| < 0.005$, respectively.

DOI: 10.1103/PhysRevD.92.094025 PACS numbers: 14.65.Ha, 12.60.Fr, 13.40.Em, 11.30.Er

I. INTRODUCTION

The recent discovery of a Higgs boson with a mass of 125 GeV in the LHC [1,2] has confirmed that the Standard Model (SM) is the theory that correctly describes electroweak interactions. However, in the context of the SM, there are many unsolved problems; among them one can mention (a) the fermion mass hierarchy, where the top quark is much heavier than other fermions, being the heaviest particle with a mass around the symmetry breaking scale, and (b) *CP* symmetry breaking in the Cabibbo-Kobayashi-Maskawa (CKM) matrix cannot explain the matter antimatter problem and the fermionic electric moments. These issues make very important the study of new sources of *CP* violation beyond the SM.

On the other hand, top quark physics is a relevant scenario for the study of physics beyond the SM [3]. In the next LHC run, at $\sqrt{s} = 14$ TeV, millions of top pairs will be produced, giving a great opportunity for the study of top quark properties, including its couplings to the gauge fields and providing an excellent scenario for new physics searches.

In the SM, top quark magnetic and chromomagnetic dipole moments (MDM and CMDM) are induced at one loop level; on the other hand, top quark anomalous electric and chromoelectric dipole moments (EDM and CEDM) appear only at three loop level, arising from the complex phase in the CKM matrix. This couplings are important in the study of new physics; in order to generate them, extended models with new sources of *CP* violation are required. This anomalous couplings sensitively affect top pair production in pp collisions. Indirect bounds to the top quark MDM have been found from the bottom quark radiative decay $b \to s\gamma$ [4,5], and also semileptonic B meson decays $(B \to Kl^+l^-)$ have been used to improve indirect bounds to MDM and EDM [6].

Since anomalous top quark couplings (ttg) affect the top production, they have been widely studied at hadron colliders. Anomalous couplings have been studied in top pair production [7–14], top pair plus jets [15], direct photon production [16], and single top production [17]. Also, spin correlations in top pair production have been used in the study of CMDM [18]. Constraints to CMDM and CEDM from Higgs boson production at the LCH have also been reported [19].

Anomalous moments have been calculated in different new physics scenarios as in the case of the MSSM [20], two Higgs doublet model (THDM) [21], little Higgs model [22], and unparticles [23]. CMDM and CEDM are defined through the effective Lagrangian

$$\mathcal{L} = \bar{u}(t)\frac{-g_s}{2m_t}\sigma_{\mu\nu}G^{\mu\nu a}T^a(\Delta\tilde{\kappa} + i\gamma_5\Delta\tilde{d})u(t), \qquad (1)$$

where $\Delta\tilde{\kappa}$ and $\Delta\tilde{d}$ represent the CMDM and CEDM, respectively; $G^{\mu\nu a}$ is the gluon field strength; and T^a are the QCD fundamental generators of $\mathrm{SU}(3)_c$.

[*]rgaitan@unam.mx
[†]egarces@fis.cinvestav.mx
[‡]josehalim@gmail.com
[§]remartinezm@unal.edu.co

In a recent study by the CMS Collaboration, spin correlation in $t\bar{t}$ cross section is used to obtain a new bound to CMDM; the bound found is $\mathrm{Re}(\Delta\tilde{\kappa}) = 0.037 \pm 0.041$, at 95% C.L., or equivalently $-0.045 < \mathrm{Re}(\Delta\tilde{\kappa}) < 0.119$ [24]. The given bound is obtained in the dilepton channel in pp collisions at $\sqrt{s} = 7$ TeV with an integrated luminosity of 5 fb^{-1} and is compared with the SM theoretical prediction, including a new physics contribution. Bounds to the top quark CMDM and CEDM are found from combined results from Tevatron and LHC (ATLAS) using high values of the $m_{t\bar{t}}$ cross section, and the bounds reported are $|\Delta\tilde{\kappa}| < 0.05$ and $\Delta\tilde{d} < 0.16$ at 95% C.L. [6]. It is estimated that in order to find a 5σ upper bound of $\Delta\tilde{d} < 0.05$ an integrated luminosity of 10 fb^{-1} at $\sqrt{s} = 13$ TeV at the LHC is required [8].

From CLEO data in the radiative decay $b \to s\gamma$, a strong constraint of $-0.03 < |\Delta\tilde{\kappa}| < 0.01$ is obtained [21]. The SM prediction to the CMDM is $\Delta\tilde{\kappa} \sim 5.6 \times 10^{-2}$ [25]. The top quark CEDM and CMDM induce new contributions to the lightest quarks through the renormalization group equations; therefore, the neutron dipole moment gives an indirect bound to the CEDM $|\Delta\tilde{d}| < 1.9 \times 10^{-3}$ [6].

In the present work, we want to study the THDM Type-III contribution, without imposing a Z_2 discrete symmetry, in the quark top CMDM and CEDM. This kind of model explicitly violates the CP symmetry in the scalar potential, which generates the top quark CMDM at one loop level. Explicit CP violation generates mixing among the neutral CP-odd and CP-even scalar fields. This mixing is very suppressed by the recent data obtained for $R_{\gamma\gamma}$ in the LHC, for the Higgs physics [26]. Using the allowed region $\alpha_1 - \alpha_2$ from the neutral scalar sector, we find the allowed values for the top quark CDMD and CEDM.

II. TWO HIGGS DOUBLET MODEL WITH *CP* VIOLATION

The simplest extension of the SM, with one extra scalar doublet is called the two Higgs doublet model; the model contains two doublet fields, Φ_1 and Φ_2; this kind of model has the advantage of being capable of describing the phenomenon of CP violation [27]. When a discrete symmetry is imposed, there are two kind of models: in the so-called Type-I, one doublet gives mass to all quarks, and in the Type-II model, one doublet gives mass to the up quarks while the other one gives mass to the down quarks. In a theory without the restriction of a discrete symmetry, also called THDM Type III, the two doublets simultaneously give mass to the up and down quarks, and the mass matrix depends on the Yukawa couplings which cannot be simultaneously diagonalized, allowing the presence of flavor changing at tree level [28].

If we consider a general THDM, the scalar potential can be written as

$$\begin{aligned} V = & -\mu_1^2\Phi_1^+\Phi_1 - \mu_2^2\Phi_2^+\Phi_2 - [\mu_{12}^2\Phi_1^+\Phi_2 + \mathrm{H.c.}] \\ & + \frac{1}{2}\lambda_1(\Phi_1^+\Phi_1)^2 + \frac{1}{2}\lambda_2(\Phi_2^+\Phi_2)^2 + \lambda_3(\Phi_1^+\Phi_1)(\Phi_2^+\Phi_2) \\ & + \lambda_4(\Phi_1^+\Phi_2)(\Phi_2^+\Phi_1) \\ & + \left[\frac{1}{2}\lambda_5(\Phi_1^+\Phi_2)^2 + \lambda_6(\Phi_1^+\Phi_1)(\Phi_1^+\Phi_2)\right. \\ & \left. + \lambda_7(\Phi_2^+\Phi_2)(\Phi_1^+\Phi_2) + \mathrm{H.c.}\right], \end{aligned} \tag{2}$$

where μ_1^2, μ_2^2, λ_1, λ_2, λ_3, and λ_4 are real parameters and the parameters μ_{12}^2, λ_5, λ_6, and λ_7 can have complex values allowing the explicit CP violation in the potential. The neutral components in the fields are defined as $\frac{1}{\sqrt{2}}(v_a + \eta_a + i\chi_a)$, where $a = 1, 2$. The vacuum expectation values (VEVs) can be taken real because complex phases can be reabsorbed in the complex parameters in the scalar potential. The VEVs take the values

$$\langle\Phi_1\rangle = \frac{1}{\sqrt{2}}\begin{pmatrix} 0 \\ v_1 \end{pmatrix}, \tag{3}$$

$$\langle\Phi_2\rangle = \frac{1}{\sqrt{2}}\begin{pmatrix} 0 \\ v_2 \end{pmatrix}. \tag{4}$$

Due to the explicit CP symmetry breaking, there will be mixing among the CP-odd and CP-even scalar sectors. Defining $\tan\beta = \frac{v_1}{v_2}$, we take the scalar field $(\eta_3 = -\chi_1 s_\beta + \chi_2 c_\beta)$ orthogonal to the would-be Goldstone component corresponding to the Z gauge boson. After symmetry breaking, the mass eigenstates of the neutral Higgs bosons are related to the η_j states as

$$h_i = \sum_{j=1}^{3} R_{ij}\eta_j, \tag{5}$$

where $i = 1, 2, 3$ and the R matrix is given by [28]

$$R = \begin{pmatrix} c_1c_2 & s_1c_2 & s_2 \\ -(c_1s_2s_3 + s_1c_3) & c_1c_3 - s_1s_2s_3 & c_2s_3 \\ -c_1s_2c_3 + s_1s_3 & -(c_1s_3 + s_1s_2c_3) & c_2c_3 \end{pmatrix}, \tag{6}$$

where the abbreviations $c_i = \cos\alpha_i$ and $s_i = \sin\alpha_i$, with $i = 1, 2, 3$, are used. h_i eigenstates do not have a well-defined CP state. For convenience, we choose

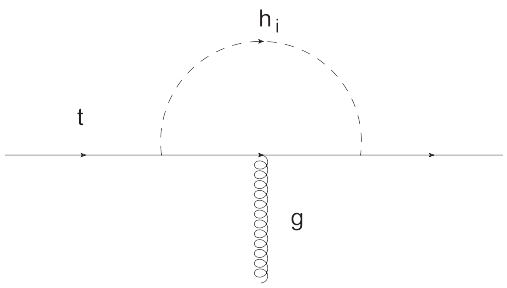

FIG. 1. Feynman Diagram for the anomalous quark-gluon couplings in the general THDM.

the neutral Higgs bosons h_i to satisfy the mass hierarchy $m_{h_1} \leq m_{h_2} \leq m_{h_3}$. In the limit case when $s_2 = s_3 = 0$, we recover the THDM without CP violation.

The Yukawa Lagrangian for the quark sector has the general form

$$-\mathcal{L}_{\text{Yukawa}} = \sum_{i,j=1}^{3}\sum_{a=1}^{2}(\bar{q}^0_{Li}Y^{0u}_{\text{aij}}\tilde{\Phi}_a u^0_{Rj} + \bar{q}^0_{Li}Y^{0d}_{\text{aij}}\Phi_a d^0_{Rj} + \text{H.c.}). \tag{7}$$

In the above equation, $Y^{u,d,l}_a$ are the 3×3 Yukawa matrices. q_L denotes the left-handed quark doublets, and u_R, d_R represent the right-handed quark singlets under $SU(2)_L$. After spontaneous symmetry breaking, the mass matrix can be written as

$$M^{u,d} = \sum_{a=1}^{2}\frac{v_a}{\sqrt{2}}Y^{u,d}_a, \tag{8}$$

where $Y^f_a = V^f_L Y^{0f}_a (V^f_R)^\dagger$, for $f = u$, d, and $V^f_{L,R}$ are the rotation matrices that diagonalize the mass matrix. The Yukawa matrix Y^u_2 as a function of M^u and Y^a_1 gives the THDM-II Lagrangian, with tree level flavor changing. For the up sector, the Yukawa Lagrangian can be written as

$$-\mathcal{L}_Y = \frac{1}{v\sin\beta}\sum_{ijk}\bar{u}_i M^u_{ij}(A^u_k P_L + A^{*u}_k P_R)u_j h_k + \frac{1}{\sin\beta}\sum_{ijk}\bar{u}_i Y^u_{ij}(B^u_k P_L + B^{*u}_k P_R)u_j h_k, \tag{9}$$

where

$$A^u_k = R_{k2} - iR_{k3}\cos\beta,$$
$$B^u_k = R_{k1}\sin\beta - R_{k2}\cos\beta + iR_{k3}. \tag{10}$$

The Y_{ij} also gives a contribution to the anomalous couplings CEDM and CMDM which is of the same order of the one in the THDM II coming from $(\bar{u}_i M^u_{ij}(A^u_k P_L + A^{*u}_k P_R)u_j h_k)$. If we asume the Cheng–Sher parametrization [29], where $(Y_{tt} \simeq m_t/v)$, both contributions must be taken into account in order to compute $\Delta\tilde{\kappa}$ y $\Delta\tilde{d}$.

III. CMDM AND CEDM IN THE GENERAL THDM

The anomalous couplings contributions for the CMDM $\Delta\tilde{\kappa}$ and for the CEDM delta $\Delta\tilde{d}$, arising from the diagram in Fig. 1, are given by the following expressions:

$$\Delta\tilde{\kappa} = \frac{G_F m_t^2}{2\sqrt{2}\pi^2\sin^2\beta}\sum_{i=1}^{3}\int_0^1 dx\int_0^{1-x}dy\frac{1}{(x+y)^2-(x+y-1)\hat{m}^2_{h_i}}[(x+y)(x+y-1)(R^2_{i2}-\cos^2\beta R^2_{i3}) - (x+y)(R^2_{i2}+\cos^2\beta R^2_{i3})], \tag{11}$$

$$\Delta\tilde{d} = -\frac{G_F m_t^2}{\sqrt{2}\pi^2\sin^2\beta}\sum_{i=1}^{3}\int_0^1 dx\int_0^{1-x}dy\frac{(x+y)(x+y-1)}{(x+y)^2-(x+y-1)\hat{m}^2_{h_i}}[\cos\beta R_{i3}R_{i2}], \tag{12}$$

where m_1, m_2, and m_3 are the masses of the h_1, h_2, and h_3, respectively. In these calculations we have used the method presented in Refs. [5,21,23].

The contribution from the Y_{ij} is

$$\Delta\tilde{\kappa}_{tt} = \frac{G_F m_t^2}{2\sqrt{2}\pi^2\sin^2\beta}\sum_{i=1}^{3}\int_0^1 dx\int_0^{1-x}dy\frac{1}{(x+y)^2-(x+y-1)\hat{m}^2_{h_i}} \times[(x+y)(x+y-1)((R_{i1}\sin\beta - R_{i2}\cos\beta)^2 - R^2_{i3}) - (x+y)[(R_{i1}\sin\beta - R_{i2}\cos\beta)^2 + R^2_{i3}]], \tag{13}$$

and for the CEDM we have

$$\Delta\tilde{d}_{tt} = -\frac{G_F m_t^2}{\sqrt{2}\pi^2\sin^2\beta}\sum_{i=1}^{3}\int_0^1 dx\int_0^{1-x}dy\frac{(x+y)(x+y-1)}{(x+y)^2-(x+y-1)\hat{m}^2_{h_i}}(R_{i1}\sin\beta - R_{i2}\cos\beta)R_{i3}. \tag{14}$$

The contributions for the CMDM and CEDM from the coupling proportional to M^u in one vertex and Y^u in the other vertex are given by

$$\Delta\tilde{\kappa}_{\text{int}} = \frac{G_F m_t^2}{2\sqrt{2}\pi^2\sin^2\beta}\sum_{i=1}^{3}\int_0^1 dx\int_0^{1-x}dy\frac{1}{(x+y)^2-(x+y-1)\hat{m}^2_{h_i}}[(x+y)(x+y-1)((R_{i1}\sin\beta - R_{i2}\cos\beta)R_{i2} + R^2_{i3}\cos\beta) - (x+y)((R_{i1}\sin\beta - R_{i2}\cos\beta)R_{i2} - R^2_{i3}\cos\beta)], \tag{15}$$

and

$$\Delta\tilde{d}_{\text{int}} = -\frac{G_F m_t^2}{\sqrt{2}\pi^2\sin^2\beta}\sum_{i=1}^{3}\int_0^1 dx\int_0^{1-x}dy\frac{(x+y)(x+y-1)}{(x+y)^2-(x+y-1)\hat{m}^2_{h_i}}[(x+y)(x+y-1)(R_{i2}R_{i3} - (R_{i1}\sin\beta - R_{i2}\cos\beta)R_{i3}\cos\beta) - (x+y)(R_{i2}R_{i3} + (R_{i1}\sin\beta - R_{i2}\cos\beta)R_{i3}\cos\beta)]. \tag{16}$$

TABLE I. M_{H^+} and $\tan\beta$ in each region.

	α_1	α_2	M_{H^+} (GeV)	$\tan\beta$
R_1	$0.67 \le \alpha_1 \le 0.8$	$0 \le \alpha_2 \le 0.23$	300	1
R_2	$0.8 \le \alpha_1 \le 1.14$	$-0.25 \le \alpha_2 \le 0.$	300	1
R_3	$1.18 \le \alpha_1 \le 1.55$	$-0.51 \le \alpha_2 \le 0$	500	1
R_4	$-1.57 \le \alpha_1 \le -1.3$	$-0.46 \le \alpha_2 \le 0.$	350	1.5
R_5	$0.93 \le \alpha_1 \le 1.57$	$-0.61 \le \alpha_2 \le 0.$	350	1.5
R_6	$-1.57 \le \alpha_1 \le -1.28$	$-0.38 \le \alpha_2 \le 0.$	350	2
R_7	$1.08 \le \alpha_1 \le 1.57$	$-0.46 \le \alpha_2 \le 0.$	350	2
R_8	$-1.39 \le \alpha_1 \le -1.3$	$-0.13 \le \alpha_2 \le 0.$	350	2.5
R_9	$1.16 \le \alpha_1 \le 1.5$	$-0.43 \le \alpha_2 \le -0.1$	350	2.5

We are using the Cheng–Sher parametrization of $Y_{tt} = m_t/v$ in Eqs. (11)–(16). We denote the total contribution as $\Delta\tilde{\kappa}_t = \Delta\tilde{\kappa} + \Delta\tilde{\kappa}_{tt} + \Delta\tilde{\kappa}_{\rm int}$ and $\Delta\tilde{d}_t = \Delta\tilde{d} + \Delta\tilde{d}_{tt} + \Delta\tilde{d}_{\rm int}$. The charged Higgs contribution to $\Delta\tilde{\kappa}$ and $\Delta\tilde{d}$ can be neglected because in the loop circulates a bottom quark and it is suppressed compared to the loop contribution in the neutral scalar sector where a top quark is the circulating particle. For the second and third terms in the sum of Eqs. (11)–(16), we considered $m_{h_2} = m_{h_3} = m_{H^+}$. In this partially degenerate case, there is CP violation for $\alpha_2 \neq 0$ [30].

We will study nine regions of interest in the α_1–α_2 parameter space; these approximate regions are described in Table I and are those already under consideration by the authors in previous work [31]. The allowed regions $R_{1..9}$ in the α_1-α_2 plane are defined from experimental bounds in $R_{\gamma\gamma}$ [32], where $R_{\gamma\gamma}$ is given by

$$R_{\gamma\gamma} = \frac{\sigma(gg \to h_1)\mathrm{Br}(h_1 \to \gamma\gamma)}{\sigma(gg \to h_{\rm SM})\mathrm{Br}(h_{\rm SM} \to \gamma\gamma)}. \tag{17}$$

Because the charged Higgs contributes to the loop in $h_1 \to \gamma\gamma$, the chosen values of $M_{H^\pm}$ and $\tan\beta$ affect the allowed region in α_1-α_2. The process $(B \to X_s\gamma)$ contains an important contribution from the charged Higgs; this

TABLE II. Range of values taken by the anomalous CMDM and CEDM. The first row shows only the contributions of $\Delta\tilde{\kappa}$ and $\Delta\tilde{d}$ according to Fig. 2. The regions in Fig. 3, which correspond to the addition of the Y^u contribution, are shown in the second row. The last row shows the regions for the three contributions based on Fig. 4.

R	CMDM	CEDM
R_1	$-1.42 \times 10^{-2} \le \Delta\tilde{\kappa} \le -1.33 \times 10^{-2}$	$0. \le \Delta\tilde{d} \le 2.41 \times 10^{-4}$
	$-2.73 \times 10^{-2} \le \Delta\tilde{\kappa}_t \le -2.63 \times 10^{-2}$	$0. \le \Delta\tilde{d}_t \le 4.56 \times 10^{-4}$
	$-2.76 \times 10^{-2} \le \Delta\tilde{\kappa}_t \le -2.50 \times 10^{-2}$	$-1.26 \times 10^{-3} \le \Delta\tilde{d}_t \le 0.$
R_2	$-1.67 \times 10^{-2} \le \Delta\tilde{\kappa} \le -1.42 \times 10^{-2}$	$-5.30 \times 10^{-4} \le \Delta\tilde{d} \le 0.$
	$-3.06 \times 10^{-2} \le \Delta\tilde{\kappa}_t \le -2.37 \times 10^{-2}$	$-5.15 \times 10^{-4} \le \Delta\tilde{d}_t \le 0.$
	$-2.50 \times 10^{-2} \le \Delta\tilde{\kappa}_t \le -1.67 \times 10^{-2}$	$0. \le \Delta\tilde{d}_t \le 2.65 \times 10^{-3}$
R_3	$-1.72 \times 10^{-2} \le \Delta\tilde{\kappa} \le -1.40 \times 10^{-2}$	$-1.61 \times 10^{-3} \le \Delta\tilde{d} \le 0.$
	$-3.03 \times 10^{-2} \le \Delta\tilde{\kappa}_t \le -2.43 \times 10^{-2}$	$-6.63 \times 10^{-4} \le \Delta\tilde{d}_t \le 0.$
	$-1.35 \times 10^{-2} \le \Delta\tilde{\kappa}_t \le -6.25 \times 10^{-3}$	$0. \le \Delta\tilde{d}_t \le 5.13 \times 10^{-3}$
R_4	$-1.18 \times 10^{-2} \le \Delta\tilde{\kappa} \le -1.11 \times 10^{-2}$	$0. \le \Delta\tilde{d} \le 7.48 \times 10^{-4}$
	$-2.35 \times 10^{-2} \le \Delta\tilde{\kappa}_t \le -2.14 \times 10^{-2}$	$-3.12 \times 10^{-4} \le \Delta\tilde{d}_t \le 0.$
	$-9.84 \times 10^{-3} \le \Delta\tilde{\kappa}_t \le -5.91 \times 10^{-3}$	$-4.36 \times 10^{-3} \le \Delta\tilde{d}_t \le 0.$
R_5	$-8.89 \times 10^{-3} \le \Delta\tilde{\kappa} \le -1.22 \times 10^{-2}$	$-7.36 \times 10^{-4} \le \Delta\tilde{d} \le 0.$
	$-1.79 \times 10^{-2} \le \Delta\tilde{\kappa}_t \le -2.23 \times 10^{-2}$	$-8.23 \times 10^{-4} \le \Delta\tilde{d}_t \le 0.$
	$-1.80 \times 10^{-2} \le \Delta\tilde{\kappa}_t \le -6.33 \times 10^{-3}$	$0. \le \Delta\tilde{d}_t \le 5.15 \times 10^{-3}$
R_6	$-9.83 \times 10^{-3} \le \Delta\tilde{\kappa} \le -9.59 \times 10^{-3}$	$0 \le \Delta\tilde{d} \le 4.49 \times 10^{-4}$
	$-1.94 \times 10^{-2} \le \Delta\tilde{\kappa}_t \le -1.79 \times 10^{-2}$	$-2.69 \times 10^{-4} \le \Delta\tilde{d}_t \le 0.$
	$-9.71 \times 10^{-3} \le \Delta\tilde{\kappa}_t \le -5.62 \times 10^{-3}$	$-3.45 \times 10^{-3} \le \Delta\tilde{d}_t \le 0.$
R_7	$-1.03 \times 10^{-2} \le \Delta\tilde{\kappa} \le -8.30 \times 10^{-3}$	$0 \le \Delta\tilde{d} \le -4.78 \times 10^{-4}$
	$-1.84 \times 10^{-2} \le \Delta\tilde{\kappa}_t \le -1.58 \times 10^{-2}$	$-5.11 \times 10^{-4} \le \Delta\tilde{d}_t \le 0.$
	$-1.59 \times 10^{-2} \le \Delta\tilde{\kappa}_t \le -6.99 \times 10^{-3}$	$0. \le \Delta\tilde{d}_t \le 3.98 \times 10^{-3}$
R_8	$-9.13 \times 10^{-3} \le \Delta\tilde{\kappa} \le -9.01 \times 10^{-3}$	$0. \le \Delta\tilde{d} \le 1.30 \times 10^{-4}$
	$-1.74 \times 10^{-2} \le \Delta\tilde{\kappa}_t \le -1.71 \times 10^{-2}$	$-9.02 \times 10^{-5} \le \Delta\tilde{d}_t \le 0.$
	$-7.93 \times 10^{-3} \le \Delta\tilde{\kappa}_t \le -6.55 \times 10^{-3}$	$-1.23 \times 10^{-3} \le \Delta\tilde{d}_t \le 0.$
R_9	$-9.30 \times 10^{-3} \le \Delta\tilde{\kappa} \le -7.87 \times 10^{-3}$	$-3.65 \times 10^{-4} \le \Delta\tilde{d} \le -1.04 \times 10^{-4}$
	$-1.63 \times 10^{-2} \le \Delta\tilde{\kappa}_t \le -1.48 \times 10^{-2}$	$-3.97 \times 10^{-4} \le \Delta\tilde{d}_t \le -1.84 \times 10^{-5}$
	$-1.44 \times 10^{-2} \le \Delta\tilde{\kappa}_t \le -8.0 \times 10^{-3}$	$8.31 \times 10^{-4} \le \Delta\tilde{d}_t \le 3.59 \times 10^{-3}$

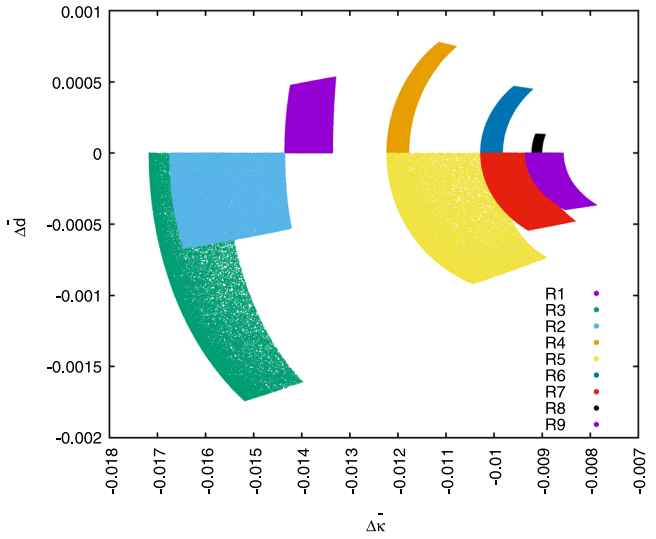

FIG. 2 (color online). Scatter plot in the $\Delta\tilde{\kappa}$ and $\Delta\tilde{d}$ plane with random values of the angles α_1, α_2 in the range allowed for each region, and $\alpha_3 = 0.$, $\tan\beta$, and M_{H^+} are as defined in Table I in every region.

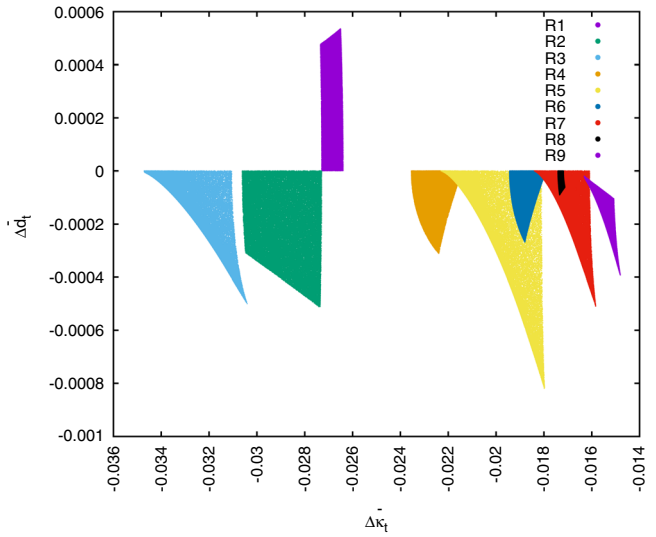

FIG. 3 (color online). Scatter plot in the $\Delta\tilde{\kappa}_t$ and $\Delta\tilde{d}_t$ plane with random values of the angles α_1, α_2 in the range allowed for each region, and $\alpha_3 = 0.$, $\tan\beta$, and M_{H^+} are as defined in Table I in every region. In this case we plot $\Delta\tilde{d}_t$ and $\Delta\tilde{\kappa}_t$ including the Y_{tt} contribution.

process strongly restricts $M_{H^\pm}$ vs $\tan\beta$ [26]. For small values of $\tan\beta$, the bound to the charged Higgs mass is of around 300 GeV [33]. A global analysis of B decays restricts $M_{H^\pm} < 400$ GeV and $\tan\beta < 10$ [34–36].

In Table I are shown the R_i regions for the given values of M_{H^+} and $\tan\beta$. In each region we set the masses of the neutral Higgses m_{h_2} and m_{h_3} equal to the mass of the charged Higgs $m_{h_2} = m_{h_3} = M_{H^+}$.

Using $(0.5 \leq R_{\gamma\gamma} \leq 2.0)$, $M_{H^\pm} = 300$ GeV, and $\tan\beta = 1.0$, the allowed regions in the α_1-α_2 plane are R_1 and R_2.

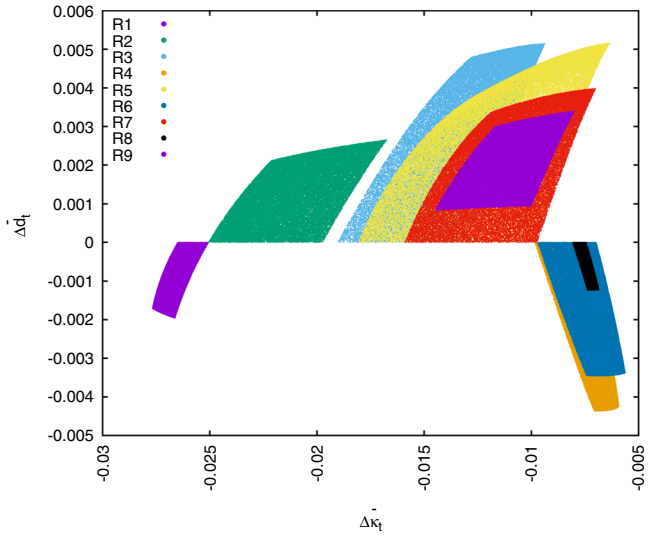

FIG. 4 (color online). Scatter plot in the $\Delta\tilde{\kappa}_t$ and $\Delta\tilde{d}_t$ plane with random values of the angles α_1, α_2 in the range allowed for each region, and $\alpha_3 = 0.$, $\tan\beta$, and M_{H^+} are as defined in Table I in every region. In this case we plot $\Delta\tilde{d}_t$ and $\Delta\tilde{\kappa}_t$ including the Y_{tt} contribution and also the interference contribution.

For the same values in the other parameters and setting the charged Higgs mass to $M_{H^\pm} = 500$ GeV, region R_3 is obtained. Combining $(1 \leq R_{\gamma\gamma} \leq 2.0)$ with $M_{H^\pm} = 350$ GeV and $\tan\beta = 1.5$, the allowed region for α_1-α_2 gives R_4 and R_5. When $\tan\beta = 2$ and for the same values to the other parameters as in $R_{4,5}$, we get $R_{6,7}$. Finally if $\tan\beta = 2.5$ the allowed regions are $R_{8,9}$.

In Table II we present the limits obtained for $\Delta\tilde{\kappa}_t$ and $\Delta\tilde{d}_t$ (or $\Delta\tilde{\kappa}$ and $\Delta\tilde{d}$) in a general THDM. To illustrate the limits reported in Table II, we show in Figs. 2, 3, and 4 the limits obtained for the anomalous moments, with values of the alpha parameters allowed for each region. To estimate the contribution of each term, we separately analyze different cases. In Fig. 2 only the contributions from Eqs. (11) and (12) are considered; meanwhile in Fig. 3 the contribution from Y^u, Eqs. (13) and (14), to previous values shown in Fig. 2 is added. All the contributions, including the interference terms (15) and (16), are considered in Fig. 4.

IV. CONCLUSIONS

In this work we have studied regions of interest in the α_1-α_2 parameter space, in order to calculate the contribution to the top anomalous couplings CMDM and CEDM in the context of a general THDM with CP violation. In our analysis, we have considered the contribution of the Yukawa coupling Y_{tt} using $M_{H^+} = 300$, 350 GeV and $\tan\beta = 1$, 1.5, 2, 2.5. We find for the nine regions of interest that the value for $\Delta\tilde{\kappa}$ can be at most of order 10^{-2} and $\Delta\tilde{d}$ of order 10^{-4}. The contributions arising from the interference of M^u and Y_u have been considered in the results. The contributions of $\Delta\tilde{\kappa}_t$ are added coherently, and

for the three contributions, the variations are not appreciable for the different regions R_i, $i = 1, \ldots, 9$. However, the contribution of $\Delta\tilde{d}_t$ coming from the interference increases almost an order of magnitude for the regions R_i, and in some cases the sign is changed.

The recent next-to-leading-order calculation for top quark production including anomalous top quark CMDM reports the bound $-0.0096 < \Delta\tilde{\kappa} < 0.0090$ [13]; our result for region R_7 is in agreement with this stringent constraint. We can also compare our theoretical bounds with those obtained from Higgs boson production at the LHC where more conservative model independent bounds are obtained [19]; our results in all nine regions are in agreement even with the most restrictive bounds projected at 14 TeV, $-0.016 < \Delta\tilde{\kappa} < 0.008$ and $|\Delta\tilde{d}| < 0.007$, as reported in Table II of Ref. [19].

With future LHC measurements at higher energy, there will be an excellent chance to probe new physics properties of the top quark; anomalous dipole moments are a measure of these new physics properties that can also give some insight in the top quark structure. A precise measurement of the top quark CMDM and CEDM, expected soon after future LHC results, will be a useful source of information in order to discriminate among different SM extensions.

ACKNOWLEDGMENTS

This work is supported in part by Programa Interno de Apoyo a Proyectos de Investigación in Facultad de Estudios Superiores Cuautitlán UNAM, Sistema Nacional de Investigadores in Mexico. J. H. Montes de Oca is thankful for support from the postdoctoral CONACYT grant. R. M. thanks to COLCIENCIAS for the financial support. E. A. G. thanks *Programa de Becas Postdoctorales en la UNAM* and a postdoctoral CONACYT grant. The authors thank L. Diaz-Cruz for useful comments on the manuscript.

[1] G. Aad *et al.* (ATLAS Collaboration), Phys. Lett. B **716**, 1 (2012).
[2] S. Chatrchyan *et al.* (CMS Collaboration), Phys. Lett. B **716**, 30 (2012).
[3] S. Y. Ayazi, H. Hesari, and M. M. Najafabadi, Phys. Lett. B **727**, 199 (2013).
[4] J. L. Hewett and T. G. Rizzo, Phys. Rev. D **49**, 319 (1994).
[5] R. Martinez and J. A. Rodriguez, Phys. Rev. D **55**, 3212 (1997).
[6] J. F. Kamenik, M. Papucci, and A. Weiler, Phys. Rev. D **85**, 071501 (2012); **88**, 039903(E) (2013).
[7] S. K. Gupta and G. Valencia, Phys. Rev. D **81**, 034013 (2010).
[8] S. K. Gupta, A. S. Mete, and G. Valencia, Phys. Rev. D **80**, 034013 (2009).
[9] D. Atwood and A. Soni, Phys. Rev. D **45**, 2405 (1992).
[10] D. Atwood, A. Kagan, and T. G. Rizzo, Phys. Rev. D **52**, 6264 (1995).
[11] Z. Hioki and K. Ohkuma, Eur. Phys. J. C **65**, 127 (2010).
[12] Z. Hioki and K. Ohkuma, Phys. Rev. D **88**, 017503 (2013).
[13] D. B. Franzosi and C. Zhang, Phys. Rev. D **91**, 114010 (2015).
[14] S. S. Biswal, S. D. Rindani, and P. Sharma, Phys. Rev. D **88**, 074018 (2013).
[15] K. m. Cheung, Phys. Rev. D **53**, 3604 (1996).
[16] H. Hesari and M. Mohammadi Najafabadi, Phys. Rev. D **91**, 057502 (2015).
[17] T. G. Rizzo, Phys. Rev. D **53**, 6218 (1996).
[18] K. m. Cheung, Phys. Rev. D **55**, 4430 (1997).
[19] A. Hayreter and G. Valencia, Phys. Rev. D **88**, 034033 (2013).
[20] J. M. Yang and C. S. Li, Phys. Rev. D **54**, 4380 (1996).
[21] R. Martinez and J. A. Rodriguez, Phys. Rev. D **65**, 057301 (2002).
[22] Q. H. Cao, C. R. Chen, F. Larios, and C.-P. Yuan, Phys. Rev. D **79**, 015004 (2009).
[23] R. Martinez, M. A. Perez, and O. A. Sampayo, Int. J. Mod. Phys. A **25**, 1061 (2010).
[24] S. Chatrchyan *et al.* (CMS Collaboration), Report No. CMS-PAS-TOP-14-005, 2014.
[25] R. Martinez, M. A. Perez, and N. Poveda, Eur. Phys. J. C **53**, 221 (2008).
[26] J. Walsh (*BABAR* and Belle Collaborations), arXiv:1412.4946.
[27] G. C. Branco, P. M. Ferreira, L. Lavoura, M. N. Rebelo, M. Sher, and J. P. Silva, Phys. Rep. **516**, 1 (2012).
[28] I. F. Ginzburg and M. Krawczyk, Phys. Rev. D **72**, 115013 (2005).
[29] T. P. Cheng and M. Sher, Phys. Rev. D **35**, 3484 (1987).
[30] A. W. El Kaffas, W. Khater, O. M. Ogreid, and P. Osland, Nucl. Phys. **B775**, 45 (2007).
[31] R. Gaitán, R. Martinez, J. H. Montes de Oca, and S. R. Romo, Eur. Phys. J. C **74**, 2788 (2014).
[32] L. Basso, A. Lipniacka, F. Mahmoudi, S. Moretti, P. Osland, G. M. Pruna, and M. Purmohammadi, J. High Energy Phys. 11 (2012) 011.
[33] S. Chatrchyan *et al.* (CMS Collaboration), Report No. CMS-PAS-HIG-12-052 (2012).
[34] A. Arbey, M. Battaglia, F. Mahmoudi, and D. Martínez Santos, Phys. Rev. D **87**, 035026 (2013).
[35] U. Haisch and F. Mahmoudi, J. High Energy Phys. 01 (2013) 061.
[36] S. Chatrchyan *et al.* (CMS Collaboration), Report No. CMS-PAS-HIG-12-011 (2012).